Efficient Inverted Tin-based Perovskite Solar Cells via Bidentate Coordination Effect of 8-Hydroxyquinoline

Zhuojia Lin[a,b], Cong Liu[a,b], Gengling Liu[a,b], Jia Yang[a,b], Licheng Tan[a,b], Yiwang Chen*[a,b]*

Z. Lin, C. Liu, G. Liu, J. Yang, Prof. Dr. L. Tan, Prof. Dr. Y. Chen

[a]College of Chemistry, Nanchang University, 999 Xuefu Avenue, Nanchang 330031, China

[b]Institute of Polymers and Energy Chemistry (IPEC), Nanchang University, 999 Xuefu Avenue, Nanchang 330031, China

Corresponding author. Tel.: +86 791 83968703; Fax: +86 791 83969561; E-mail: ywchen@ncu.edu.cn (Y. C.); tanlicheng@ncu.edu.cn (L. T.).

Experimental Section

Materials: Indium-tin oxide (ITO) glass (the sheet resistance of 15 Ω per sq and the transmittance of 86%) was purchased from South China Xiang Science and Technology Company, Ltd. PEDOT:PSS (aqueous dispersion, Clevios VP AI 4083) was obtained from Heraeus. Formamidinium iodide (FAI) (anhydrous, 99.99%), Tin (II) iodide (SnI_2, 99.99%), tin (II) fluoride (SnF_2, 99%), and bathocuproine (BCP, 96.0%), N,N-dimethylformamide (DMF, anhydrous, 99.8%), dimethyl sulfoxide (DMSO, anhydrous, 99.9%), and chlorobenzene (CB, anhydrous, 99.8%) were purchased from Sigma-Aldrich. PCBM (99%) was acquired from Xi'an Polymer Light Technology Corp.

Device Fabrication: The ITO glass substrates were ultrasonically cleaned by detergent, acetone, deionized water, and isopropyl alcohol for 15 min in series and finally were treated by oxygen plasma for 5 min. Then, the PEDOT:PSS solution was spin-coated onto the ITO substrates at 4000 rpm for 1min, followed by annealing at 140 °C for 20 min. The precursor solution was prepared by dissolving 1 M FAI, 1 M SnI_2, and 0.1 M SnF_2 in 800 μL DMF and 200 μL DMSO with different mass fraction

of 8-Hydroxyquinoline to total mass of FAI and SnI_2 in glovebox. The perovskite films were obtained by one-step method: the substrates were spun at 5000 rpm for 30s in glovebox, after 50 μL $FASnI_3$ precursor solution was dropped on ITO/ PEDOT:PSS substrates. CB was dripped as the anti-solvent in the 9th second and the perovskite film was annealed at 95 °C for 15 min. Next, the $PC_{61}BM$ (20 mg/mL in CB) was spin-coated onto the perovskite film at 2000 rpm for 30 s. Finally, BCP (8nm) and Ag(100nm) layer were sequentially evaporated under a vacuum level of 10^{-4} Pa. The active area of this device is 0.04cm^2.

Characterization: X-ray photoelectron spectroscopy (XPS) were performed on the Thermo Scientific ESCA Lab 250Xi with perovskite films coated on ITO substrates. The prepared solution was subjected to Shimadzu IRPrestige-21 spectrometer with a spectral range of 4000 to 500 cm^{-1}. Steady-state photoluminescence (PL) and time-resolved photoluminescence (TRPL) measurements were recorded by photoluminescence spectroscopy (FLS920, Edinburgh Instruments Ltd.) at a peak emission of approximately 840 nm (the excitation at 510 nm) for steady state and lifetime measurements. NMR measurements, X-ray diffraction (XRD) patterns and UV-visible (UV-Vis) spectra were measured on Bruker ADVANCE 400 MHz Spectrometer, D8-Discover 25 diffractometer (Bruker) and SHIMADZU UV-2600 spectrophotometer, respectively. Scanning electron microscopy (SEM) images of the perovskite film were obtained by JSM-7800F SEM. The J–V characteristics of the devices were acquired by Keithley 2400 with an AM 1.5G (100 mW cm^{-2}). The incident photon-to-current conversion efficiency (IPCE) spectra were measured on monochrome illumination (Oriel Cornerstone 260 1/4 m monochromator with Oriel 70613NS QTH lamp) and the incident light was calibrated by a monocrystalline silicon diode. Electrical impedance spectroscopy (EIS) analysis was acquired by Zahner electrochemical workstation. Current–voltage (I–V) curves of electron-only devices and hole-only devices were measured by using a Keithley 2400 Source Meter under dark conditions.

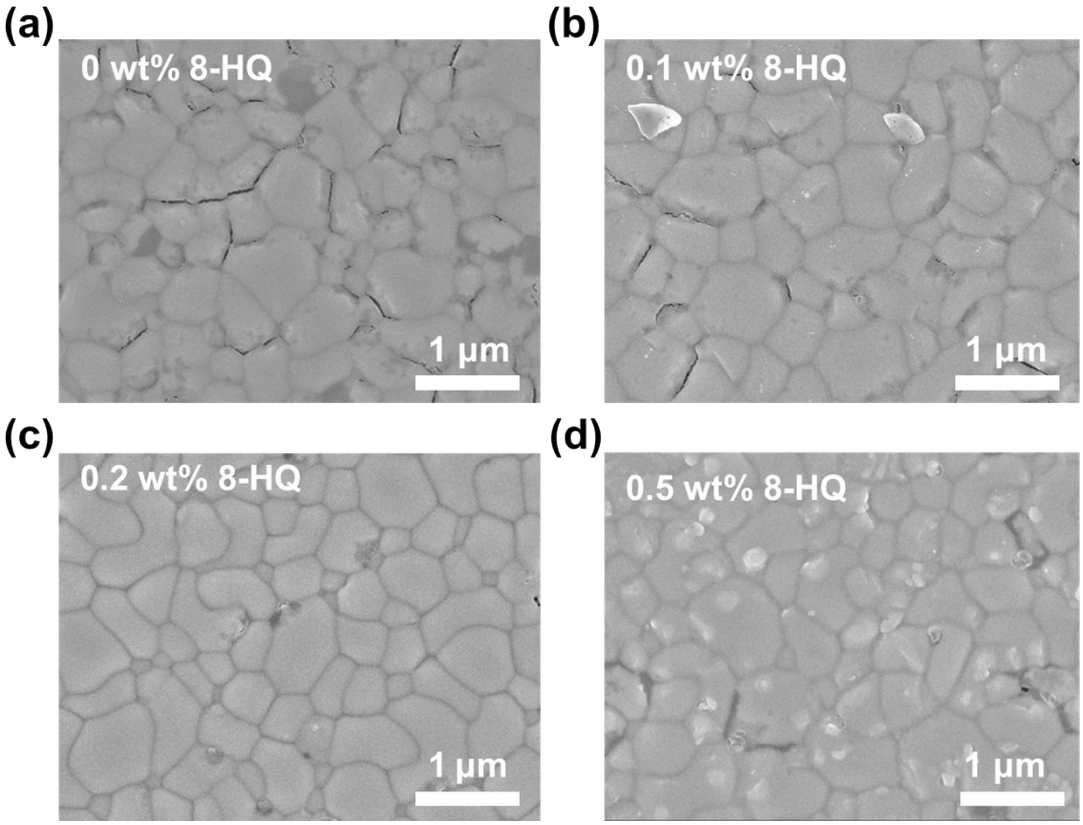

Figure S1. Scanning electron microscope (SEM) images of $FASnI_3$ perovskite films with different ratios of 8-HQ: 0 wt%, 0.1 wt%, 0.2 wt%, and 0.5 wt%.

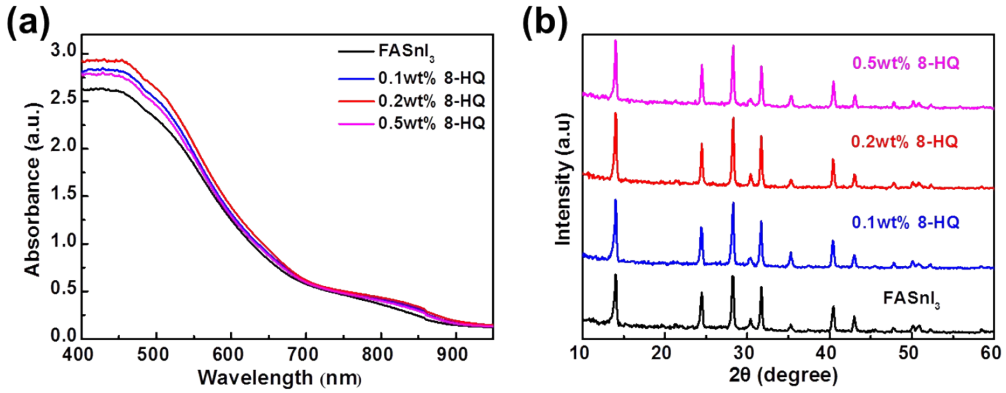

Figure S2. (a) UV-vis absorption spectra and (b) X-ray diffraction (XRD) patterns of $FASnI_3$ perovskite films with different ratios of 8-HQ: 0 wt%, 0.1 wt%, 0.2 wt%, and 0.5 wt%.

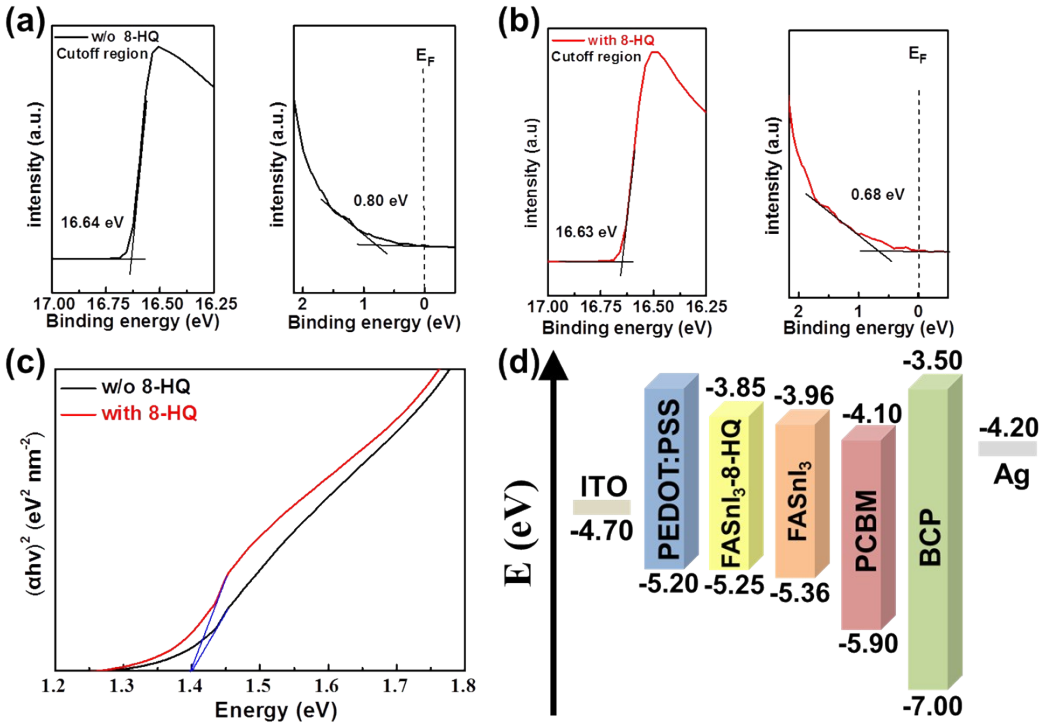

Figure S3. Ultraviolet photoelectron spectroscopy (UPS) of secondary electron cutoff and valence band for $FASnI_3$ perovskite films (a) without and (b) with 8-HQ. (c) The relationship of $(\alpha h\nu)^2$ vs energy for $FASnI_3$ films without and with 8-HQ. (d) Schematic energy level diagram of the corresponding PVSCs.

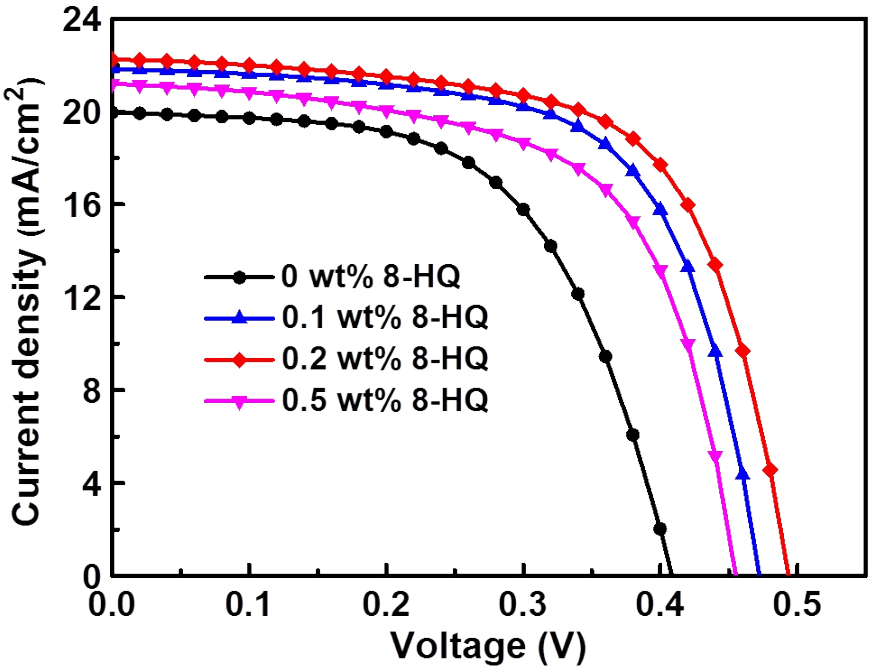

Figure S4. The current density-voltage (*J-V*) curves of $FASnI_3$-based PVSCs with different ratios of 8-HQ: 0 wt%, 0.1 wt%, 0.2 wt%, and 0.5 wt%.

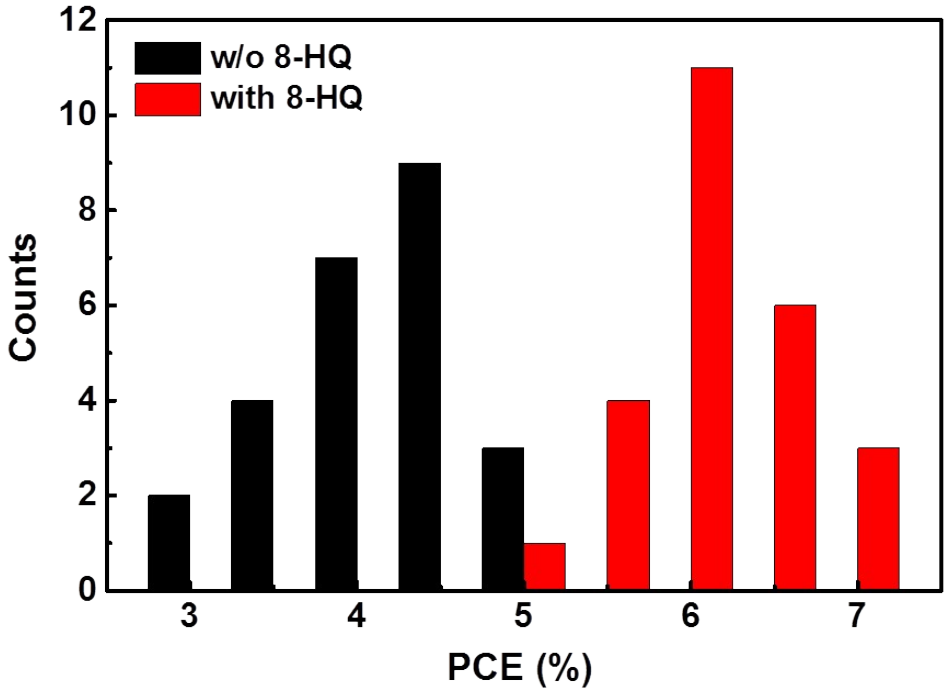

Figure S5. Histograms of PCE distribution for 25 devices based on $FASnI_3$ perovskite films (without and with 8-HQ).

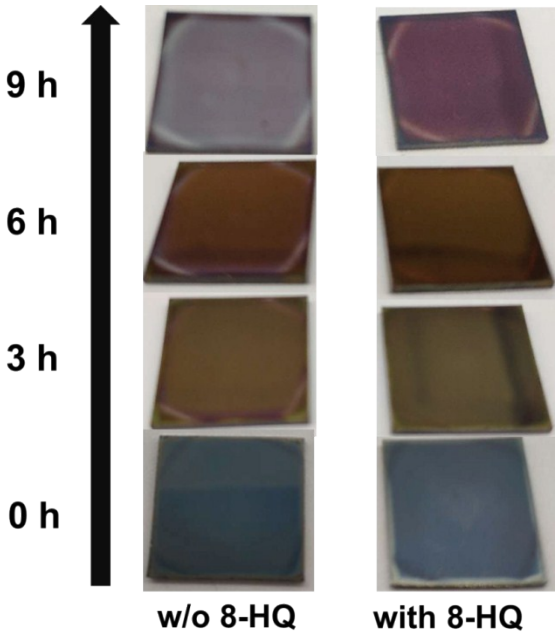

Figure S6. The photographs of $FASnI_3$ perovskite films without and with 8-HQ aged in air (50% relative humidity).

Figure S7. The water contact angle measurement on the $FASnI_3$ perovskite films (a) without and (b) with 8-HQ.

Table S1. Proportion of Sn^{2+} and Sn^{4+} in surface based on $FASnI_3$ perovskite films (without and with 8-HQ).

Sample	Sn^{2+}	Sn^{4+}
w/o 8-HQ	56.84%	43.16%
with 8-HQ	86.08%	13.92%

Table S2. The photoelectric parameters of $FASnI_3$-based PVSCs without and with 8-HQ.

Device	V_{oc} (V)	FF (%)	J_{sc} (mA/cm^2)	PCE (%)
0 wt% 8-HQ	0.40	58.22	19.95	4.74
0.1 wt% 8-HQ	0.47	64.82	21.83	6.68
0.2 wt% 8-HQ	0.49	65.19	22.24	7.15
0.5 wt% 8-HQ	0.45	62.65	20.20	5.72

Table S3. Photovoltaic parameters of 25 devices based on $FASnI_3$ perovskite films without 8-HQ.

No.	V_{oc} (V)	FF (%)	J_{sc} (mA/cm^2)	PCE (%)
1	0.408	58.22	19.95	4.74
2	0.408	59.59	18.60	4.52
3	0.384	60.18	19.46	4.50
4	0.406	60.16	18.16	4.44
5	0.384	58.96	19.41	4.40
6	0.386	59.38	18.98	4.36
7	0.372	58.50	19.74	4.30
8	0.383	57.25	19.37	4.26
9	0.394	56.14	19.17	4.25
10	0.388	57.16	18.98	4.21
11	0.381	57.80	18.57	4.09
12	0.369	60.65	17.86	4.00
13	0.361	60.68	18.17	3.97
14	0.372	56.56	18.85	3.96
15	0.363	58.53	18.39	3.91
16	0.386	57.44	17.37	3.85
17	0.366	56.99	18.27	3.82
18	0.363	55.81	18.31	3.71
19	0.358	59.87	16.42	3.53
20	0.375	54.52	16.82	3.44
21	0.351	55.88	16.98	3.38
22	0.340	57.69	16.51	3.24
23	0.355	56.01	16.19	3.21
24	0.327	50.76	18.29	2.86
25	0.326	50.24	17.24	2.71
Average	0.372±0.022	57.39±2.66	18.24±1.07	3.91±0.53

Table S4. Photovoltaic parameters of 25 devices based on $FASnI_3$ perovskite films with 8-HQ.

No.	V_{oc} (V)	FF (%)	J_{sc} (mA/cm^2)	PCE (%)
1	0.493	65.19	22.24	7.15
2	0.494	65.03	21.89	7.03
3	0.480	65.01	22.45	7.02
4	0.492	64.62	21.83	6.93
5	0.483	65.63	21.48	6.81
6	0.478	64.60	21.95	6.78
7	0.471	64.40	22.17	6.72
8	0.477	64.17	21.54	6.59
9	0.483	63.06	21.42	6.53
10	0.469	64.08	21.48	6.47
11	0.475	63.70	21.19	6.42
12	0.477	61.28	21.93	6.41
13	0.485	61.06	21.29	6.31
14	0.471	63.88	20.91	6.30
15	0.479	60.63	21.60	6.28
16	0.481	60.74	21.35	6.25
17	0.485	62.21	20.51	6.19
18	0.485	61.29	20.52	6.10
19	0.479	63.06	20.06	6.07
20	0.482	61.62	20.35	6.05
21	0.484	62.31	19.74	5.96
22	0.478	61.94	19.97	5.92
23	0.486	60.95	19.89	5.90
24	0.483	60.01	19.86	5.75
25	0.478	58.87	19.50	5.49
Average	0.481±0.006	62.77±1.87	21.08±0.88	6.37±0.42

Table S5. The trap state density and carrier mobility based on $FASnI_3$ without and with 8-HQ (hole-only and electron-only devices).

Sample	Hole-only devices			Electron-only devices		
	V_{TFL} (V)	N_t (cm^{-3})	Hole mobility ($cm^2\ V^{-1}\ s^{-1}$)	V_{TFL} (V)	N_t (cm^{-3})	Electron mobility ($cm^2\ V^{-1}\ s^{-1}$)
w/o 8-HQ	0.31	1.21×10^{16}	1.01×10^{-3}	0.25	8.25×10^{15}	2.77×10^{-2}
with 8-HQ	0.22	8.65×10^{15}	3.65×10^{-3}	0.21	9.82×10^{15}	2.85×10^{-2}